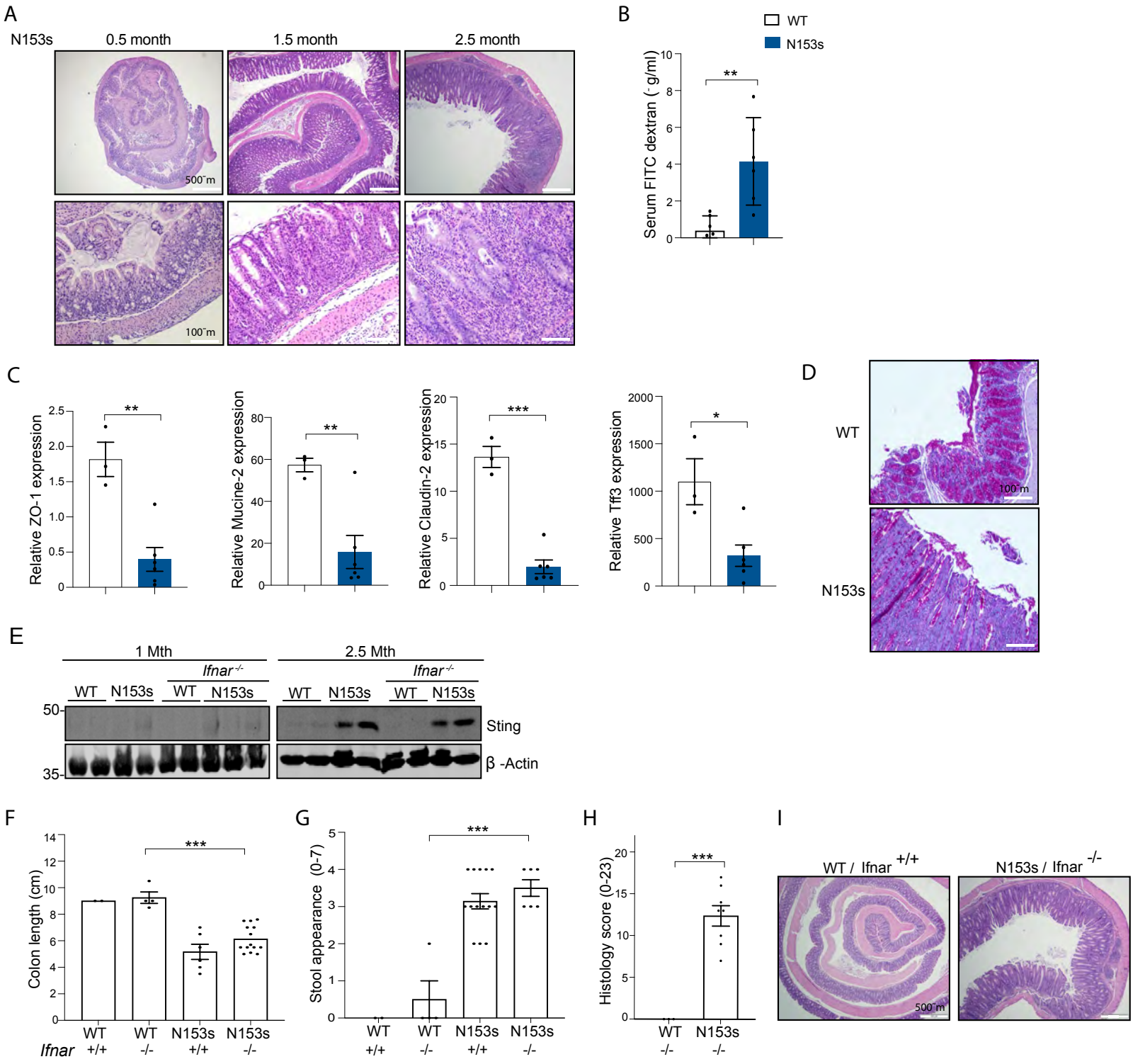

Supp Figure 1. N153s mice exhibit intestinal inflammation independently of Type I Interferon. Related to Figure. 1. (A) Representative images of H&E-stained colon section of N153s mice at the indicated age. (B) Concentration of 4-kDa FITC dextran in plasma of N153s mice 4 hours post administration by oral gavage. (C) QPCR analysis of ZO-1, Mucine-2, Claudin-2 and Tff3 mRNA expression in colon tissue samples obtained from 4.5-months old N153s and WT littermate control mice. (*P<0.05,**P<0.01,***P<0.001, Data are represented as mean ±SEM of n=2-4 from 2 independent experiments). QPCR gene expression levels were normalized to TBP (D) Representative images of PAS-stained colon section of 4.5-month of age N153s and WT littermate control mice. (E) Representative images of Western blotting detecting STING in WT, N153s and N153s deficient for type I IFN receptor (IFNAR) mice at the indicated age. (F) Colon length, (G) stool appearance and (H) pathology score of 4-month old N153s mice intercrossed to Ifnar deficient mice (***P<0.001. Data are represented as mean ±SEM of n=2-7 from 3 independent experiments). (I) Representative images of H&E stained colon section of the indicated mice.

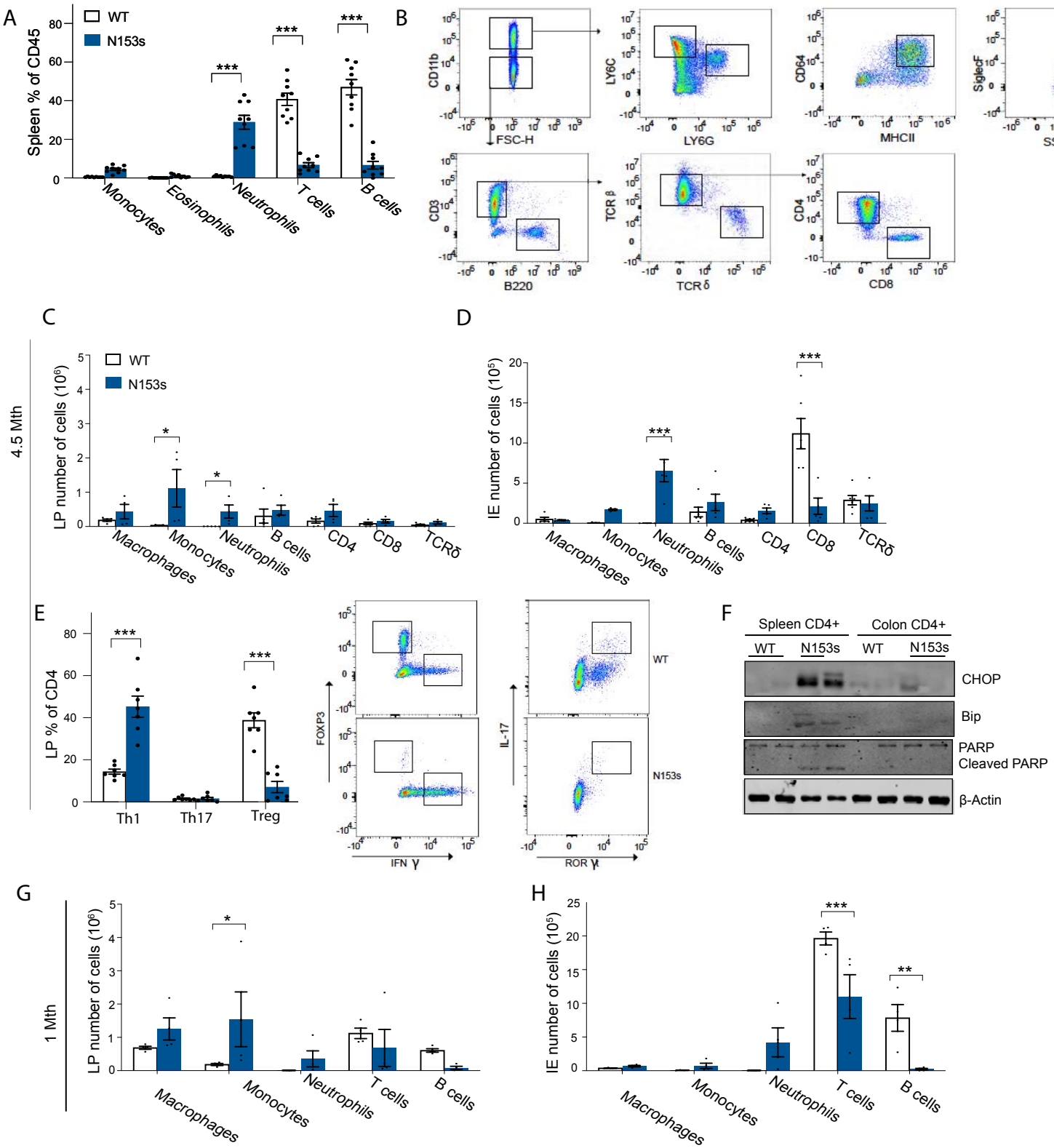

Supp Figure 2. N153s mice develop immune cell alterations in the colon and spleen. Related to Figure. 2. (A) Flow cytometry analysis of splenic immune cells presented as % out of CD45+ cells (***P<0.001. Data are represented as mean ±SEM of n=2-3 from 5 independent experiments). (B) Representative flow cytometry gating strategy of colonic LP immune cells from N153s mice. Flow cytometry analysis of colonic (C) LP and (D) IE immune cells from 4.5-month-old. (E) Flow cytometry analysis and gate strategy of LP Th1 IL-1Thi RORt+, Th1 IFNhi and Treg FOuF3hi T cells (***P<0.001. Data are represented as mean ±SEM of n=2-5 from 2 independent experiments). (F) Representative images of Western blotting detecting CHOP, Bip and cleaved PARP1 in CD4+ T cells isolated from spleen and colon of 3.5-month-old N153s and WT littermate control mice. Flow cytometry analysis of (G) LP and (H) IE immune cells from 1-month-old N153s and WT littermate control mice presented as absolute number of cells. (*P<0.05,***P<0.001, Data are represented as mean ±SEM of n=3-5 from 2 independent experiments)

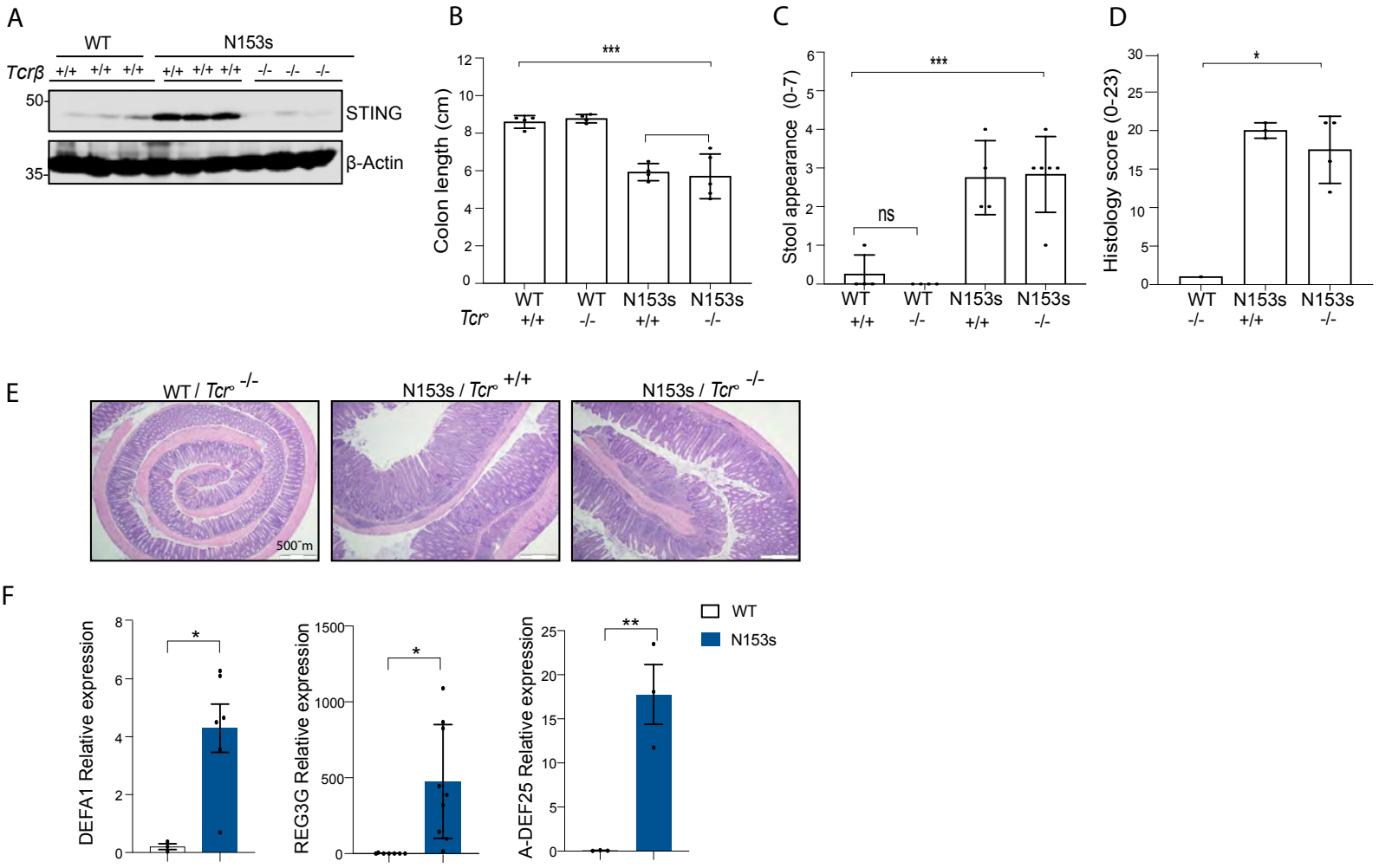

Supp Figure 3. N153s mice exhibit T cell-dependent colitis. Related to Figure 2. (A) Western blotting detecting STING in the indicated mice. (B) colon length, (C) stool appearance and (D pathology score of the indicated mice at 4-months of age. (*P<0.05,***P<0.001. Data are represented as mean ±SEM of n=3-S from 3 independent experiments). (E) Representative images of H&E-stained colon sections at 4-months of age. (F) qPCR analysis of colonic anti-microbial peptides, mRNA in 4.5-month-old N153s and WT l mice. Gene expression levels were normalìoed to TBP. (*P<0.05,**P<0.01. Data are represented as mean ±SEM of n=3-4 from 2 independent experiments).

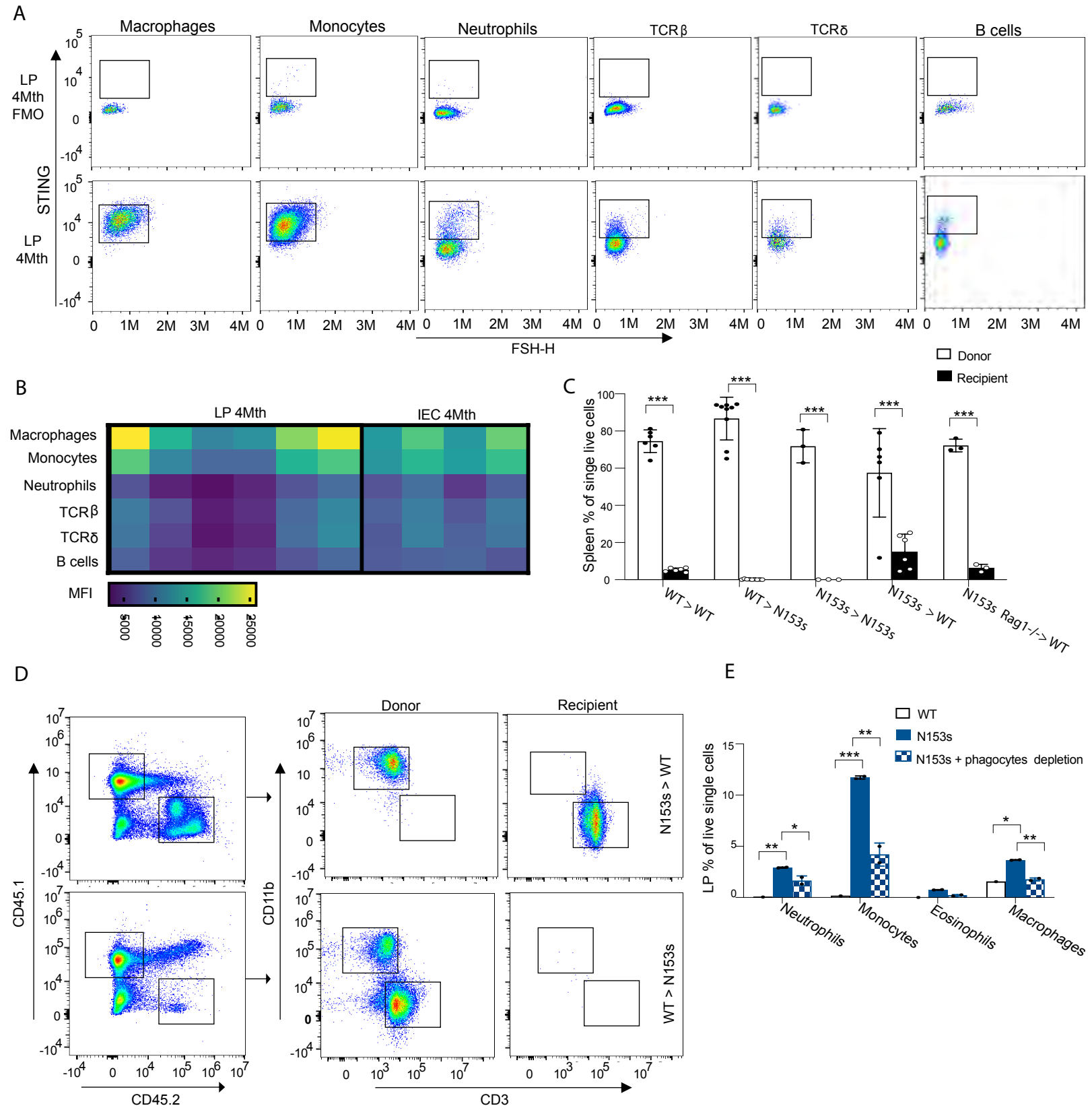

Supp Figure 4. STING accumulates in colonic myeloid cells of N153s mice. Related to Figure 3. (A) Representative flow cytometry gating strategy of colonic STING expressing LP immune cells from N153s mice at 4-months of age (lower panel). Accurate gating was determined by Fluorescent Minus One (FMO) panel lacks anti STING antibody (upper panel). (B) Heat-map representing Mean Fluorescent Intensity (MFI) of STING in colonic LP and IE immune cells of each cell subset of N153s mice at the age of 4.5-month-old, quantified by flow cytometry. **Intrinsic activation of STING in myeloid cells drives intestinal inflammation in N153s mice. Related to Figure 4.** (C) flow cytometry analysis of splenic donor and recepient cells of the indicated mice (***P<0.001. Data are represented as mean ±SEM of n=2-5 from 4 independent experiments). (D) Representative flow cytometry gating strategy of LP CD45.1 and CD45.2 cells of N153s > WT chimera mice. (E) Flow cytometry analysis of colonic myeloid cells of the indicated mice (*P<0.05, **P<0.01,***P<0.001. Data are represented as mean ±SEM of n=1-2 from 2 independent experiments).

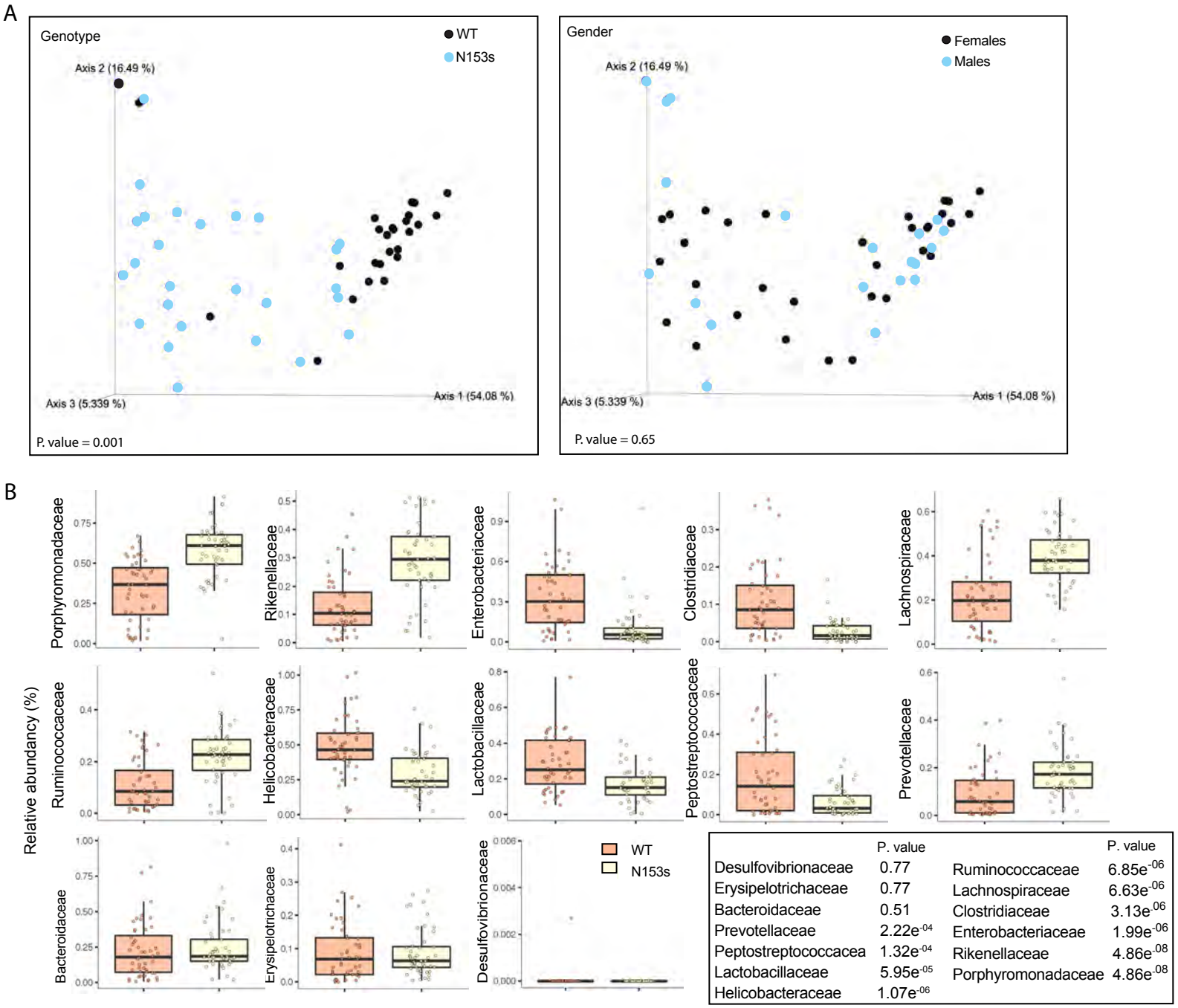

	P. value		P. value
Desulfovibrionaceae	0.77	Ruminococcaceae	$6.85e^{-06}$
Erysipelotrichaceae	0.77	Lachnospiraceae	$6.63e^{-06}$
Bacteroidaceae	0.51	Clostridiaceae	$3.13e^{-06}$
Prevotellaceae	$2.22e^{-04}$	Enterobacteriaceae	$1.99e^{-06}$
Peptostreptococcacea	$1.32e^{-04}$	Rikenellaceae	$4.86e^{-08}$
Lactobacillaceae	$5.95e^{-05}$	Porphyromonadaceae	$4.86e^{-08}$
Helicobacteraceae	$1.07e^{-06}$		

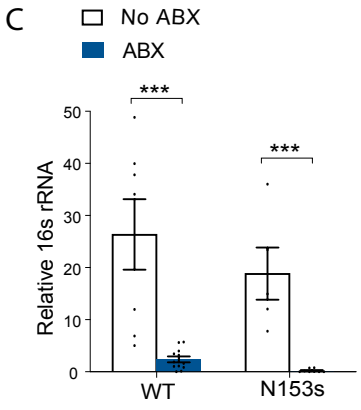

Supp Figure 5. Commensal dysbiosis drives intestinal inflammation in N153s mice. Related to Figure 5. (A) Principal coordinates analysis (PCoA) plots of 16S rDNA community profiles representing -diversity based on genotype and gender and using the weighted UniFrac distance metric; significance was tested using pairwise PERMANOVA. (B) Graphical summary of family-level, differential abundance by genotype. Significant taxa were determined using the MaAsLin2 multivariate statistical framework including both age and gender as random effect (Data are represented as mean ±SEM of n=40-48). (C) 16S rDNA gene copies as quantified by real time RT-PCR from fecal pellets collected from WT and N153s mice treated or untreated with broad spectrum antibiotic cocktail. Gene expression levels were normalized to GAPDH (Data are represented as mean ±SEM of n=5-12)

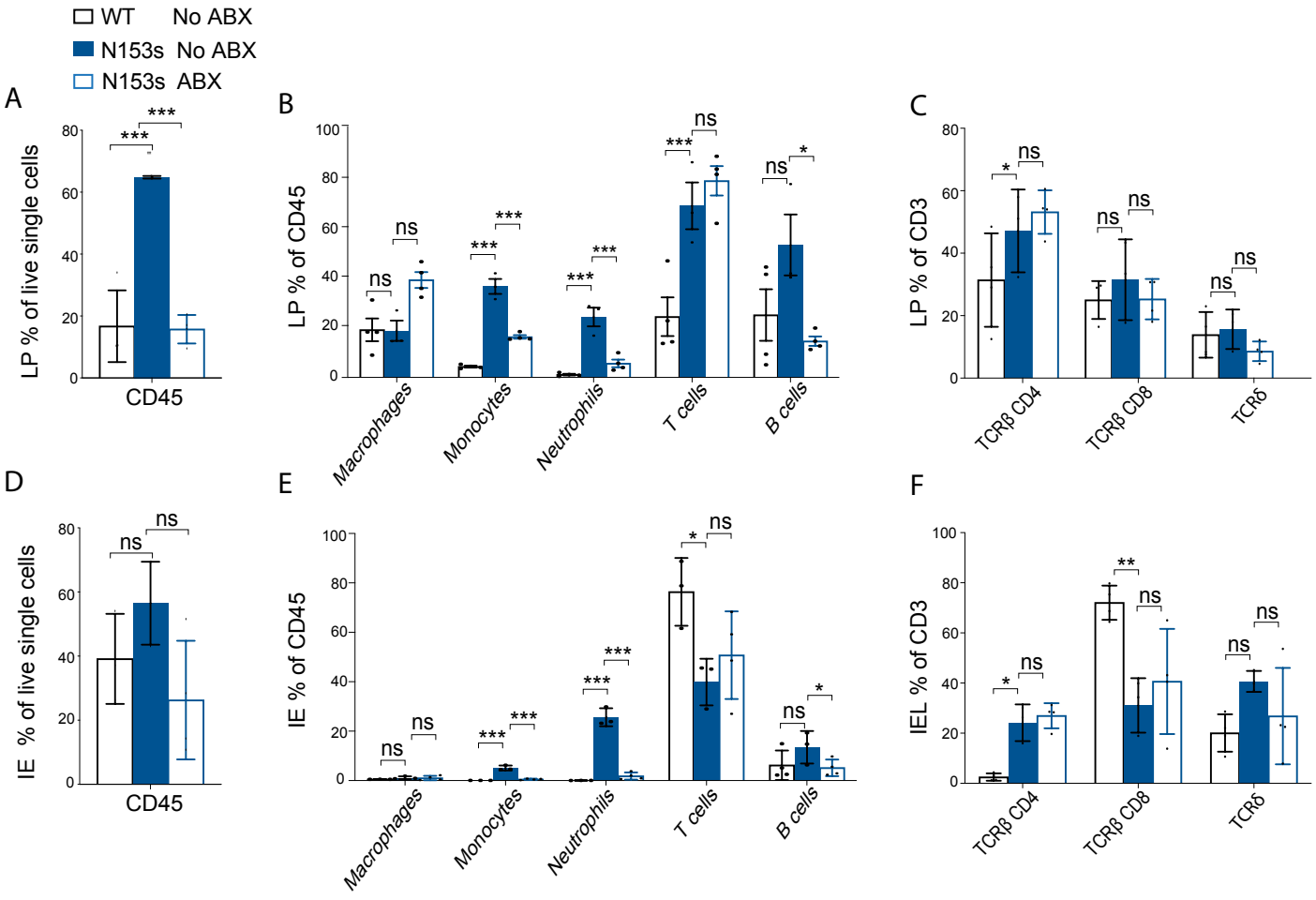

Supp Figure 6. Depletion of commensal bacteria in N153s mice alter immune cell population. Related to Figure. 6. Flow cytometry analysis of colonic LP (A-C) and IE (D-F) immune cell populations from the indicated mice. Graphical summary of LP (A) and IE (D) CD45+ cells presented as % out of live single cells. (B,E) CD11b+CD64 +MHCII+ macrophages, CD11b+Ly6Chi monocytes, CD11b+ Ly6Ghi neutrophils, CD11b- CD3+ T cells and CD11b- B200+ B cells presented as % out of CD45+ cells. (C,F) TCR CD4, TCR CD8 and TCR T cells presented as % out of CD3+ cells. (Data are represented as mean ±SEM of n=2-3 from 2 independent experiments).

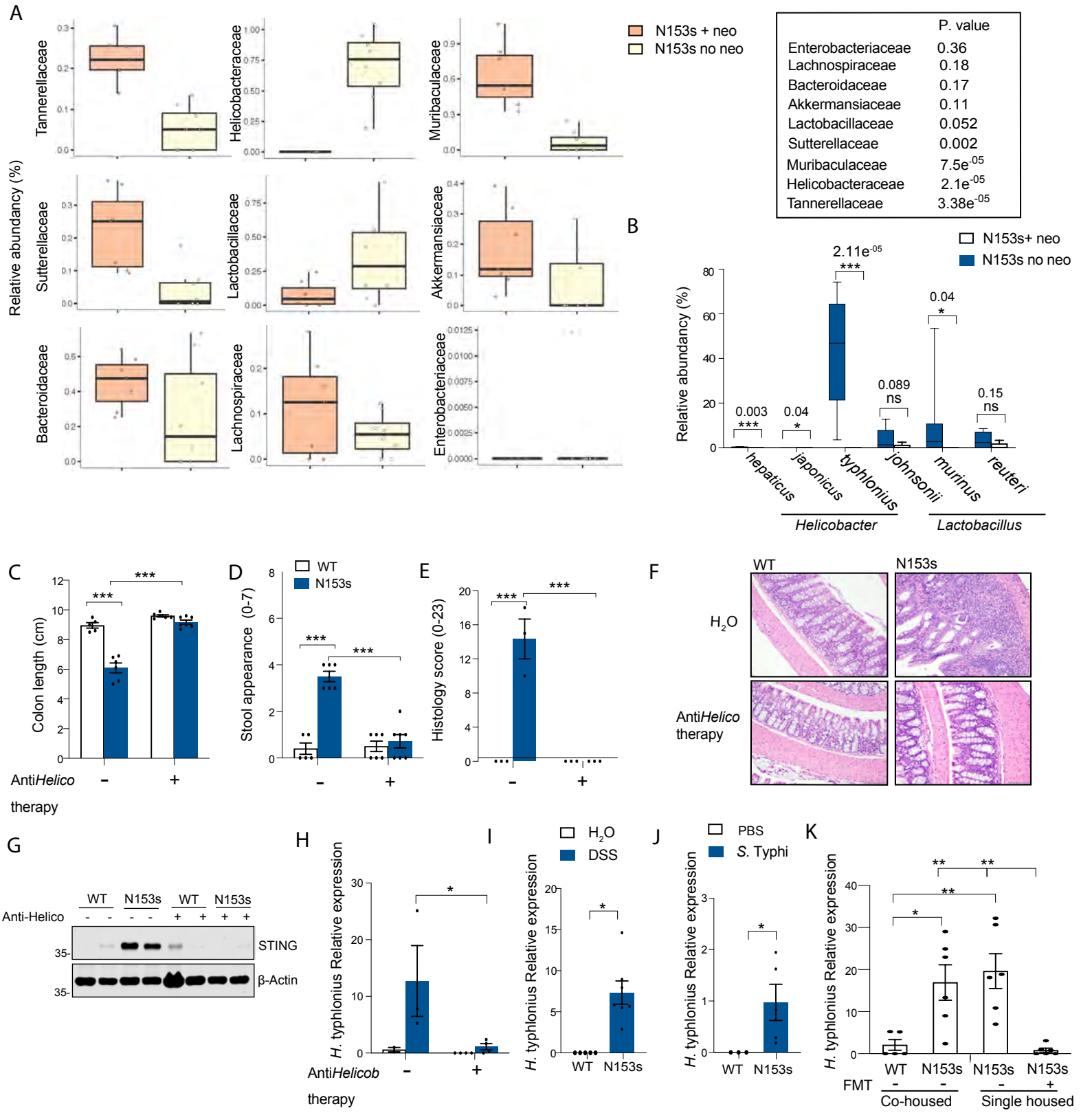

Supp Figure 7. Shotgun sequencing revealed a significant reduction of Helicobacteraceae bacteria family. Related to Figure 7. (A) Family-level relative abundance of fecal commensal flora determined by WGS. All taxa lower than 5% are indicated as "Other families". Significance assessed using MaAsLin2 multivariate statistical framework. (Data are represented as mean ±SEM of n=7-9). (B) Relative abundances at the species levels of fecal Helicobacter and Lactobacillus detected by WGS sequencing. (C) colon length, (D) stool appearance and (E) pathology score of the indicated mice. (F) H&E-stained colon sections and (G) Western blotting detecting STING in the indicated mice. (H) H. typholonlus relative expression quantified by qPCR from fecal pellets collected from the indicated mice. (*P<0.05. Data are represented as mean ±SEM of n=2 from 2 independent experiments). H. typholonlus relative expression from fecal pellets collected from (I) DSS challenged mice and (J) mice challenged with S.typhimurium and (K) the indicated mice from FMT experiment, Gene expression levels were normalized to GAPDH (Data are represented as mean ±SEM of n=2-4 from 2 independent experiments).